Materials Science in Semiconductor Processing 12 (2009) 224–232

Contents lists available at ScienceDirect

Materials Science in Semiconductor Processing

journal homepage: www.elsevier.com/locate/mssp

Electrical characterization of current conduction in Au/TiO_2/n-Si at wide temperature range

H. Altuntas *, A. Bengi, U. Aydemir, T. Asar, S.S. Cetin, I. Kars, S. Altindal, S. Ozcelik

Physics Department, Faculty of Arts and Sciences, Gazi University, 06500 Ankara, Turkey

ARTICLE INFO

Available online 29 December 2009

Keywords:
Au/TiO_2/n-Si Schottky barrier diodes
I–V characteristics
Barrier height
Inhomogeneous barrier
Gaussian distribution

ABSTRACT

In this study, we have examined Au/TiO_2/n-Si Schottky barrier diodes (SBDs), in order to interpret in detail the experimental observed non-ideal current–voltage–temperature (*I–V–T*) characteristics. *I–V* characteristics were measured in the wide temperature range of 80–400 K. TiO_2 was deposited on n-Si substrate by reactive magnetron sputtering. The zero-bias barrier height (ϕ_{B0}) and ideality factor (n) show strong temperature dependence. While n decreases, ϕ_{B0} increases with increasing temperature. Experimental results show that the current across the SBDs may be greatly influenced by the existence of Schottky barrier height (SBH) inhomogeneity. These temperature behaviors have been explained on the basis of the thermionic emission (TE) theory with Gaussian distribution (GD) of the barrier heights (BHs) due to BH inhomogeneities at metal–semiconductor (M/S) interface. From this assumptions, obtaining Richardson constant value of the A^* 121.01 A/cm^2 K^2 is perfect agreement with the theoretical value of 120 A/cm^2 K^2 for n-type Si. Hence, behaviors of the forward-bias *I–V* characteristics of the Au/TiO_2/n-Si (SBDs) can be successfully explained on the basis of a TE mechanism with a double Gaussian distribution of the BHs.

1. Introduction

The titanium dioxide (TiO_2) thin films have been extensively studied because of their low density of interface states (N_{ss}) and high dielectric constants [1–6]. It has been used in semiconductor products, i.e., sensors, photocatalysts, antireflection coatings, MOSFET gate dielectrics, and also been used for optical applications. In recent years, insulator layers forming on Si, such as Si_3N_4, SnO_2, and TiO_2 films, have been examined as a potential material to replace silicon dioxide (SiO_2). The main advantages of these films are the lower densities of the surface states and their high dielectric permittivity when compared to SiO_2. Many deposition methods can be used to prepare TiO_2 films; thermal or anodic oxidation of titanium [7,8], electron beam evaporation [9], chemical vapor deposition [10], plasma-enhanced chemical vapor deposition [11], sol–gel method [12,13], and reactive sputtering methods [14–17]. Among these methods, DC reactive magnetron sputtering method is much more preferable since it is easier to control and this method has made the fabrication of insulator films with reproducible and desired properties possible. The performance and reliability of TiO_2 based devices particularly depend on the formation of TiO_2 layer at M/S interface, the level of N_{ss} at Si/TiO_2 interface, series resistance of devices, and inhomogeneities of the Schottky barrier (SB) formation at M/S interface [18–22]. The device technology has been hindered by the very high N_{ss} between Si and TiO_2. A poor interface of the insulator film with Si leads to high leakage currents and high defect trapped charges. Therefore, implementation of the high-dielectrics on Si requires studying electrical properties of the Si/TiO_2 interface. Experimental results, especially only at room temperature

* Corresponding author. Fax: +90 312 212 2279.
E-mail address: altunhalit@gmail.com (H. Altuntas).

1369-8001/$ - see front matter © 2009 Elsevier Ltd. All rights reserved.
doi:10.1016/j.mssp.2009.12.001

or narrow range of temperature, do not give detailed information about their current-conduction mechanisms or barrier formation at the M/S interface. However, the temperature dependence of the *I–V* characteristics in the wide temperature range allows us to understand different aspects of conduction mechanisms and device characteristics [21]. Usually, the thermionic emission (TE) theory is normally used to extract the diode parameters such as the zero-bias barrier height ϕ_{B0} and ideality factor n is expected to be close to unity, similar to that observed at uniform Schottky barrier diodes. However, experimental analysis of the *I–V* characteristics of such devices based on TE mechanism usually reveals an abnormal decrease in the ϕ_{B0} and an increase in n with a decrease in temperature, which leads to non-linearity in the activation energy plots of $\ln(I_0/T^2)$ versus $1/T$ [22–26]. Recently, temperature dependence of ϕ_{B0}, n, and the non-linearity behavior of activation energy plots at low temperatures in some studies have been successfully explained on the basis of TE mechanism with Gaussian distribution [19–24,27–35]. The spatial barrier inhomogeneities in MS and MIS SBDs are described mainly by Gaussian distribution function and it has been widely accepted to correlate the experimental data [20,21,27–35].

In this study, the forward and reverse-bias current–voltage (*I–V*) characteristics of Au/TiO_2/n-Si (SBDs) have been investigated in the wide temperature range of 80–400 K. The temperature dependent barrier characteristics of the Au/TiO_2/n-Si (SBDs) were interpreted by assuming double-Gaussian spatial distribution of BHs.

2. Experimental method

Au/TiO_2/n-Si SBD structures were fabricated on a 2 in diameter float zone (1 0 0) n-type (phosphorus doped) polycrystal silicon wafer, having a thickness of 350 μm. For the fabrication process, Si wafer was degreased in organic solvent of $CHClCCl_2$, CH_3COCH_3, and CH_3OH consecutively and then etched in a sequence of H_2SO_4 and H_2O, 20% HF, a solution of $6HNO_3$:1HF:$35H_2O$, 20% HF and finally quenched in deionized water for a prolonged time. Preceding each cleaning step, the wafer was rinsed thoroughly in deionized water of resistivity of 18 MΩ cm. Substrates were clamped to a stainless steel holder provided with an optical heater. Thin films of TiO_2 were deposited by UHV reactive magnetron sputtering system using high purity (99.999%) Ti target, in varying Ar+O_2 reactive gas mixtures on n-Si substrate. Prior to film deposition, Si substrates were sputter cleaned in pure argon ambient after raising the substrate temperature to 400 °C in 10^{-8} mbar high vacuum, to ensure the removal of any residual organics. Sputtering operations were carried out with mass flow controllers. The automatic control system of gas valves was used for Ar and O_2. The flow of Ar and O_2 was maintained at 9 and 1 sccm (90% Ar–10% O_2), respectively. The film with 1500 A thickness was deposited at a constant pressure of 4.2×10^{-3} mbar and a constant substrate temperature of 200 °C. After deposition, the film was thermally treated by annealing in air atmosphere for 4 h at 400 °C.

The ohmic and rectifier contacts were formed by sintering the HV thermal deposition system in the pressure of 10^{-7} mbar with tungsten holder. High purity Au (99.999%) was evaporated onto the whole back surface of the substrate at 450 °C as a back contact, and was annealed at 400 °C to form good ohmic contact behavior. After that ~1000 Å thick Au (99.999% purity) dots of 2 mm diameter were evaporated onto TiO_2 film at 70 °C. In this way, Au/TiO_2/n-Si SBD structures were fabricated for the electrical measurements. The electrode connections were made by silver paste.

The temperature dependence of *I–V* measurements were performed by the use of a Keithley 2400 sourcemeter, a Keithley 614 electrometer in the temperature range of 80–400 K using a temperature-controlled Janes vpf-475 cryostat. The sample temperature was always monitored by using a copper-constant thermocouple close to the sample, and measured with a dmm/scanner Keithley model 199 and a Lake Shore model 321 autotuning temperature controllers with sensitivity better than ± 0.1 K. All measurements were carried out with the help of a microcomputer through an IEEE-488 ac/dc converter card.

3. Results and discussion

Semi-logarithmic forward and reverse-bias *I–V* characteristics of Au/TiO_2/n-Si SBDs at 80–400 K are shown in Fig. 1. The current through a SBD at a forward bias ($V \geq 3kT/q$), according to the TE mechanism, is given by [36–38]

$$I = I_0\left[\exp\left(\frac{qV}{nkT}\right)-1\right] \tag{1}$$

where, V is the forward bias voltage, n the ideality factor, T the temperature in K, and I_0 the reverse saturation current derived from the straight-line intercept of ln$I$ at zero bias and is given by

$$I_0 = AA^*T^2\exp(-q\phi_{B0}/kT) \tag{2}$$

where, the quantities A, A^*, q, k, T and ϕ_{B0} are the diode area, the effective Richardson constant and equals to 120 A/cm^2 K^2 for n-type Si [36], the electronic charge, the Boltzmann constant, temperature in K and the zero-bias barrier height, respectively.

In Fig. 1, the "soft" or slightly non-saturating behavior was observed as a function of bias in the reverse bias branch, which may be explained in terms of the image force lowering of Schottky barrier height [39,40] and the presence of the interfacial layer between the metal and Si wafer. Also, as can be seen Fig. 1, the forward bias *I–V* characteristics are linear in the intermediate regions but considerably deviate from linearity due to the series resistance effect of the Au/TiO_2/n-Si (SBDs) structure.

Using Eq. (1), the ideality factor n can be written as

$$n = \frac{q}{kT}\left(\frac{d(V)}{d\ln(I)}\right). \tag{3}$$

The values of the ideality factor are obtained from the slope of the linear region forward bias ln(I)–V plots. In this region, the effect of series resistance can be negligible. The

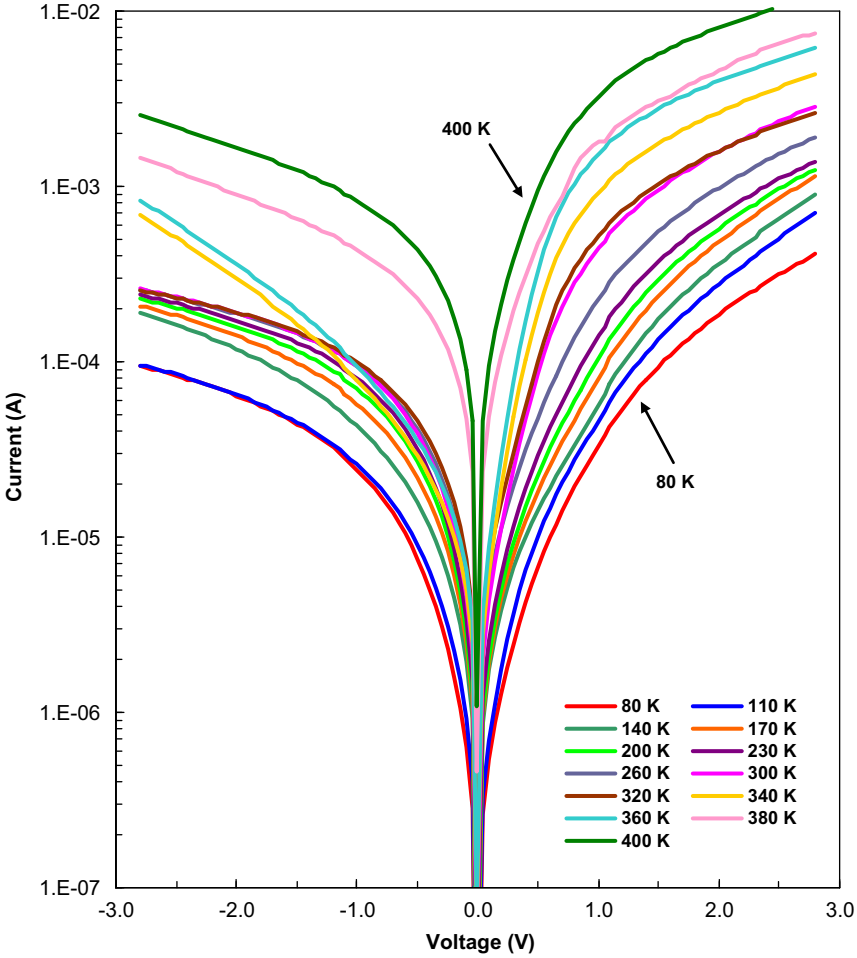

Fig. 1. The semi-logarithmic forward and reverse bias current–voltage characteristics of the Au/TiO_2/n-Si (SBD) at various temperatures.

ϕ_{B0} was calculated using theoretical value A^* (120 A/cm^2 K^2) and extrapolated I_0 at each temperature according to

$$\phi_{B0} = \frac{kT}{q} \ln\left(\frac{AA^*T^2}{I_0}\right). \quad (4)$$

Values of the n and ϕ_{B0} were calculated using the Eqs. (3) and (4), respectively, and were shown in Table 1 and Fig. 2 at various temperature. As shown in Table 1, n and ϕ_{B0} for Au/TiO_2/n-Si SBD are 7.61 and 0.18 eV at 80 K and 1.49 and 0.82 eV at 400 K, respectively. It is clear that both the values of n and ϕ_{B0} are strong functions of temperature. The high value of ideality factor n has been attributed to the effects of the bias voltage drop across the interfacial insulator layer, the particular distribution of interface states localized at semiconductor/insulator interface, and the special barrier inhomogeneities at the M/S interface [20,26,29,36,39–42].

For the evaluation of the barrier height, one may also make use of the Richardson plot of saturation current. Eq. (2) can be rewritten as

$$\ln\left(\frac{I_0}{T^2}\right) = \ln(AA^*) - \frac{q\phi_{B0}}{kT} \quad (5)$$

Table 1
The experimentally obtained characteristic parameters of the Au/TiO_2/n-Si SBDs in the temperature range of 80–400 K.

T(K)	I_o (A)	n	Φ_{B0} (eV)
80	1.26E-07	7.61	0.18
110	3.74E-07	5.92	0.24
140	1.02E-06	5.24	0.30
170	3.05E-06	4.10	0.36
200	5.30E-07	3.01	0.45
230	7.16E-07	2.43	0.52
260	1.46E-06	2.14	0.58
300	2.33E-06	1.75	0.67
220	5.29E-06	1.64	0.69
340	7.81E-06	1.71	0.73
360	9.93E-06	1.51	0.76
380	1.57E-05	1.53	0.80
400	2.25E-05	1.49	0.83

As shown in Fig. 3, the temperature dependence of $\ln(I_0/T^2)$ versus q/kT is found to be linear in two temperature ranges measured as 80–170 K and 200–400 K. Fitting the experimental data at higher temperatures (200–400 K) an activation energy value of 0.08 eV from the slope of this straight line was obtained

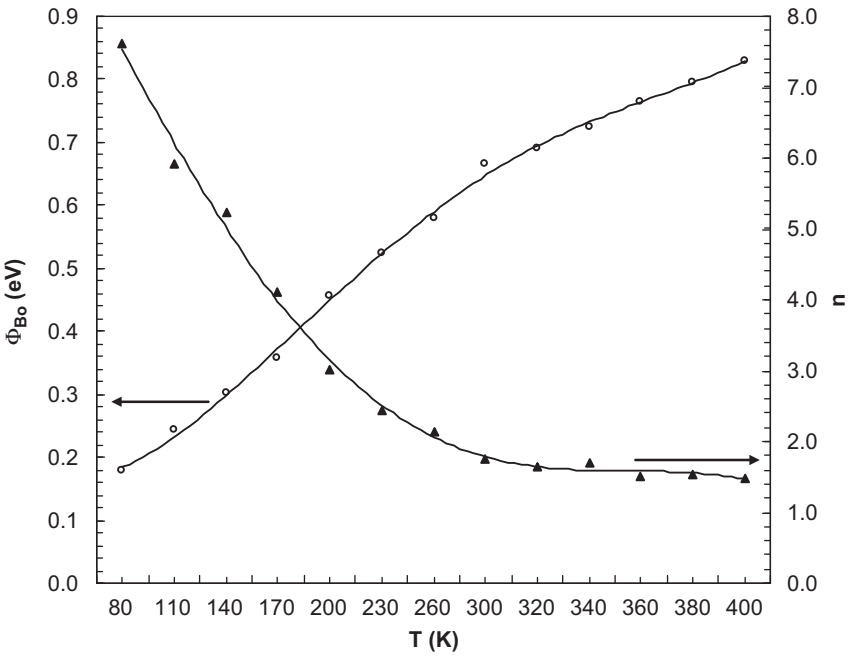

Fig. 2. The variation in the ideality factor and zero-bias barrier height with temperature for Au/TiO_2/n-Si (SBD).

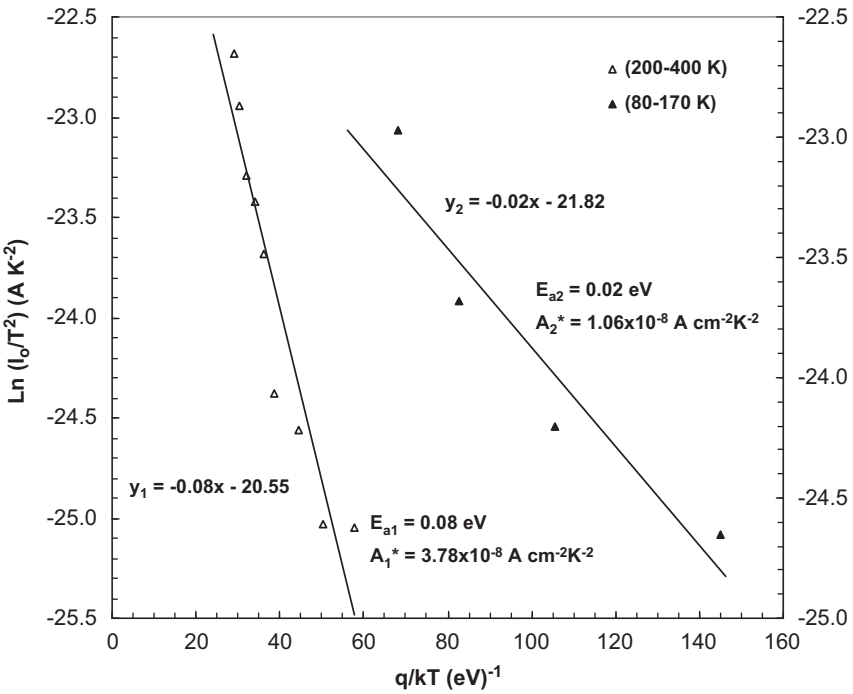

Fig. 3. Richardson plots of $\ln(I_0/T^2)$ versus q/kT for Au/TiO_2/n-Si (SBDs).

and at lower temperatures (80–170 K), 0.02 eV obtained. Likewise, Richardson constants values of 3.78×10^{-8} A/cm^{2}K^2 (200–400 K) and 1.06×10^{-8} A/cm^{2}K^2 (80–170 K) for Au/TiO_2/n-Si were obtained from the intercept at the ordinate of experimental $\ln(I_0/T^2)$ versus q/kT plot in Fig. 3. These values are much and much lower than the theoretical value of Richardson constant for n-Si that is 120 A/cm^2 K^2. This discrepancy was explained by Horvath [34] the A^* value obtained from the temperature dependence of *I–V* characteristics may be affected by the lateral inhomogeneity of the barrier.

According to Tung's theory [43], there is a linear correlation between the experimental zero bias barrier heights ϕ_{B0} and ideality factors *n*. ϕ_{B0} versus *n* was shown

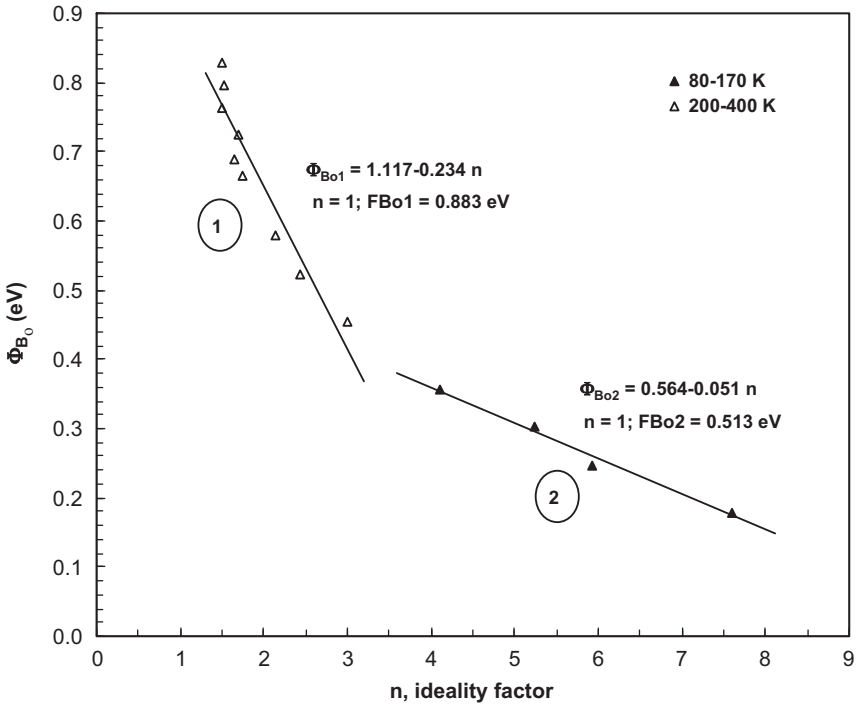

Fig. 4. ϕ_{B0} versus n of the Au/TiO_2/n-Si (SBDs) at different temperatures.

in Fig. 4. As can be seen in Fig. 4, there are two linear regions between ϕ_{B0} and n values of the Al/TiO_2/n-Si, which can be explained by the lateral inhomogeneities of the barrier heights [24,44]. In the first region (200–400 K), the extrapolation of the experimental ϕ_{B0} and n plot to $n=1$ has given the value of 0.883 eV, which is close to the band gap of Si. In the second region (80–170 K), the extrapolation of ϕ_{B0} and n plot to $n=1$ has given the value of 0.513 eV, which is close to half of the band gap of Si. This behavior indicates that, under forward bias, the current transport for $T \geq 170$ K is controlled by TE and for $T \leq 170$ K by the thermionic field emission mechanism [36,38]. These results confirm that predominant current transport is not only the TE in our SBDs. Also, these observations show the presence of two Gaussian distributions, namely, Gaussian distribution 1 (200–400 K) and Gaussian distribution 2 (80–170 K) in the contact area, because ϕ_{B0} versus n plot has two straight lines with different slopes.

As told above, the decrease in the BH with a decrease in temperature can be explained by the lateral distribution of BH if the barrier height has a Gaussian distribution over the Schottky contact area with the mean BH $\overline{\phi}_{B0}$ and standard deviation σ_s. The standard deviation is a measure of the barrier homogeneity. The Gaussian distribution of the BHs is given by [28,29,45].

$$\phi_{ap} = \overline{\phi}_{B0} - \frac{q\sigma_s^2}{2kT} \tag{6}$$

In this formula, ϕ_{B0} was changed by ϕ_{ap}, where ϕ_{ap} is the apparent barrier height measured experimentally. The temperature dependence of σ_s is usually small and can be neglected. The observed variation of the apparent ideality factor with temperature in the model is given by [28].

$$\left(\frac{1}{n_{ap}} - 1\right) = -\rho_2 + \frac{q\rho_3}{2kT} \tag{7}$$

where ρ_2 and ρ_3 quantities are the voltage coefficients, which may depend on temperature and they quantify the voltage deformation of the BH distribution. Fitting the experimental I–V data to Eqs. (3) and (4) gives ϕ_{B0} and n, respectively, which should obey Eqs. (6) and (7). Thus, the plot of ϕ_{B0} versus q/kT (Fig. 5(a)) should be a straight line with intercept at the ordinate determining the zero-bias mean BH $\overline{\phi}_{B0}$ and slope giving the zero-bias standard deviation σ_s. The experimental ϕ_{B0} versus q/kT plots (Fig. 5(a)) drawn by means of the data obtained from Fig. 2 respond to two lines with transition occurring at 170 K. The observations of two straight lines are evidence of the presence of Gaussian distribution of barrier heights in the contact area. The intercepts and slopes of these straight lines give two sets of values of $\overline{\phi}_{B0}$ and σ_s as 1.173 eV and 0.158 V in the temperature range in 200–400 K (distribution 1), and as 0.495 eV and 0.071 V in the temperature range of 80–170 K (distribution 2). The standard deviation is a measure of the barrier homogeneity. The lower value of σ_s corresponds to more homogenous barrier height.

This study shows that Au/TiO_2/n-Si Schottky diode has double Gaussian distribution. The existence of a double Gaussian in the metal–semiconductor contacts can be attributed to the nature of the inhomogeneities themselves in the two cases. This may involve variation in the interface composition/phase, interface quality, electrical charges, nonstoichiometry, etc. [47]. They are important enough to electrically influence the current–voltage (I–V)

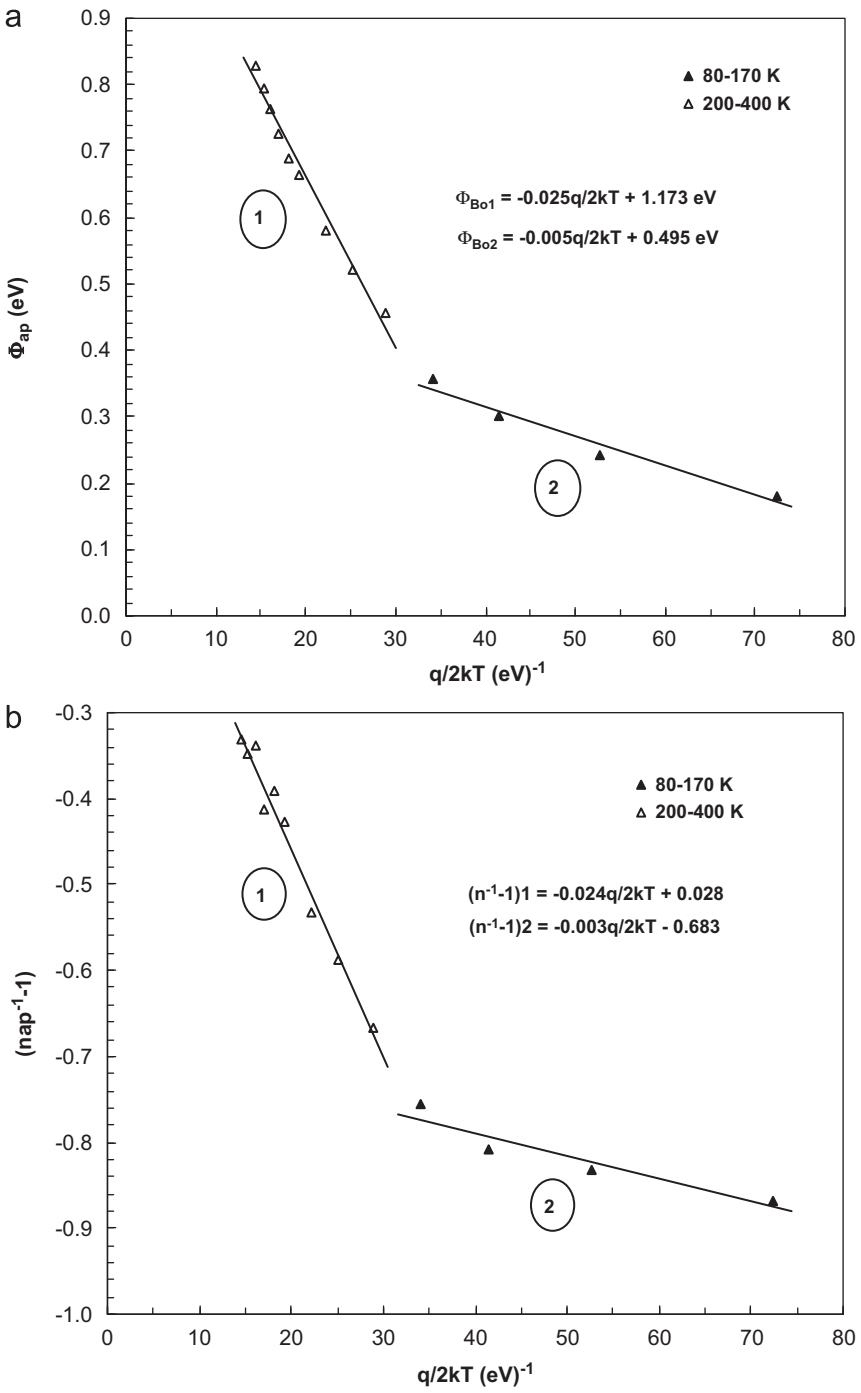

Fig. 5. Zero-bias barrier height (a) and ideality factor (b) versus $q/(2kT)$ curve of the Au/TiO_2/n-Si (SBD) according to two Gaussian distributions of BHs. The data show linear variation in the two temperature ranges with a transition around 170 K.

characteristics of the Schottky diodes, at particularly low temperatures [46]. Thus, *I–V* measurements at very low temperatures are capable of revealing the nature of barrier inhomogeneities present in the contact area. Furthermore, the temperature range covered by each straight line suggests the regime where corresponding distribution is effective.

Like this, the plot of n_{ap} versus q/kT gives different characteristics in two temperature ranges since the contacts contain two barrier height distributions. This can be clearly seen in Fig. 5(b). The intercept and slope of the straight lines in n_{ap} versus $1/T$ plot gives the voltage coefficient ρ_2 and ρ_3, respectively. The values of ρ_2 obtained from the intercepts of the experimental n_{ap}

versus q/kT plot (Fig. 5b) are -0.028 in the temperature range of 200–400 K (distribution 1), and 0.683 in the temperature range of 80–170 K (distribution 2), whereas the values of ρ_3 from the slopes are 0.024 V in 200–400 K range and 0.003 V in 80–170 K temperature ranges. The linear behavior of this plot demonstrates that the ideality factor does indeed express the voltage deformation of the Gaussian distribution of the SBH. As can be seen from Fig. 5(b), ρ_3 value or slope of distribution 1 is larger than distribution 2, therefore, we may point out that distribution 1 is a wider and relatively higher barrier height with bias coefficients ρ_2 and ρ_3 being smaller and larger, respectively.

As can be seen from Fig. 3, the conventional activation energy $\ln(I_0/T^2)$ versus q/kT plot has showed non-linearity at low temperatures. To explain these behaviors, using $\overline{\phi}_{B0}$ in place of experimental ϕ_{B0} in Eqs. (2) and (4) according to Gaussian distribution of the BH, it can be rewritten as

$$\ln\left(\frac{I_0}{T^2}\right)-\left(\frac{q^2\sigma_s^2}{2k^2T^2}\right)=\ln(AA^*)-\frac{q\overline{\phi}_{B0}}{kT} \tag{8}$$

and modified activation energy plot from this formula is obtained and given in Fig. 6.

Using the experimental I_0 data, a modified $\ln(I_0/T^2)-((q^2\sigma_s^2)/(2k^2T^2))$ versus q/kT can be obtained according to Eq. (8) and should give a straight line with slope directly yielding the mean $\overline{\phi}_{B0}$ and the intercept ($=\ln AA^*$) at the ordinate determining A^* for a given contact area. The $\ln(I_0/T^2)-((q^2\sigma_s^2)/(2k^2T^2))$ values were calculated for both values σ_s obtained for the temperature ranges of 80–170 and 200–400 K. From the straight line of these two regions, zero-bias mean BH was obtained=0.506 eV (in the range of 80–170 K) and 1.161 eV (in the range of 200–400 K). These values are very close to the mean BHs obtained from the ϕ_{ap} versus $q/2kT$ plot in Fig. 5(a). As discussed above, the intercepts at the ordinate give the Richardson constant A^* as 324.06 A/cm^2 K^2 (in 80–170 K range) and 121.01.46 A/cm^2 K^2 (in 200–400 K range) without using the temperature coefficient of the BHs. The Richardson constant value for n-Si is known as 120 A/cm^2 K^2. This theoretical value is in perfect agreement with 121.01 A/cm^2 K^2, which is obtained by approaching double Gaussian distribution.

In addition, as can be seen from Fig. 7, the double logarithmic forward bias I–V plot of the Au/TiO_2/n-Si SBD at six different temperatures were drawn to explain the current conduction mechanisms such as thermionic emission (TE) theory, space charge-limited current (SCLC), and trap-charge limited current (TCLC). Here the thickness variations of the insulator layer were assumed to be unchanged with temperature. Because the change in ideality factor and $\ln(I_0/T^2)$ versus $1/nT$ with reverse temperature are not linear behavior. Therefore, the tunneling probability for electrons and the ideality factor was not accounted in the reverse saturation current expression (in Eq. (2)). Also, it is clear that these double logarithmic forward bias I–V plots exhibit a good linearity in the bias voltage range of 0.05–0.20 V. As can be explained in Refs. [48–52], the double logarithmic forward bias I–V plots with a slope equal to 2 or larger than 2 suggest the possibility of SCLC mechanism at intermediate and high bias voltage. Such behavior of the slope has been interpreted as an indication for TCLC with an exponent trap distribution [48–53] double logarithmic forward bias I–V plots. However, the space charge formation and the density distribution nature of interface states (N_{ss}) localized at semiconductor/insulator layer

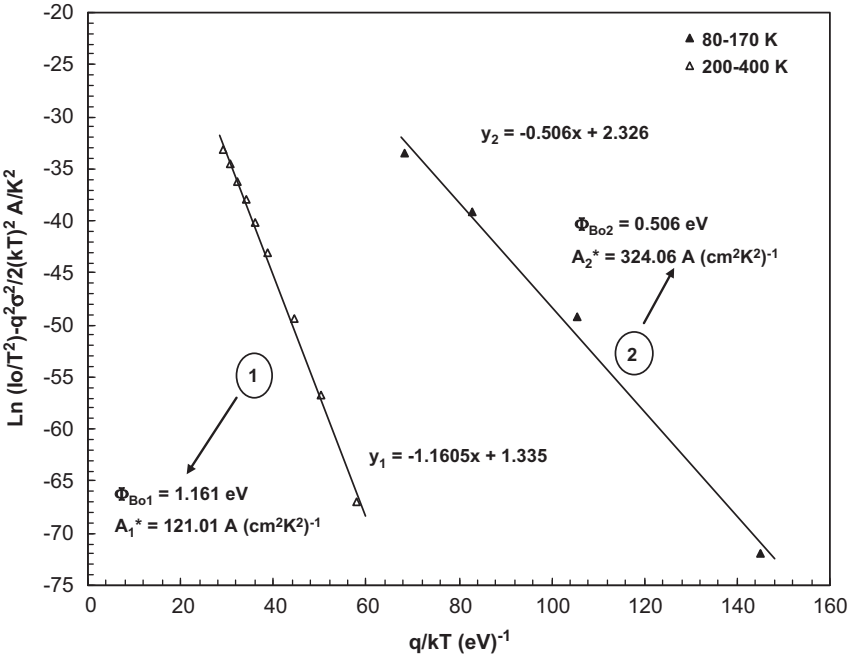

Fig. 6. Modified Richardson $\ln(I_0/T^2)-((q^2\sigma_s^2)/(2k^2T^2))$ versus q/kT plot for the Au/TiO_2/n-Si (SBD) according to Gaussian distribution of the barrier height.

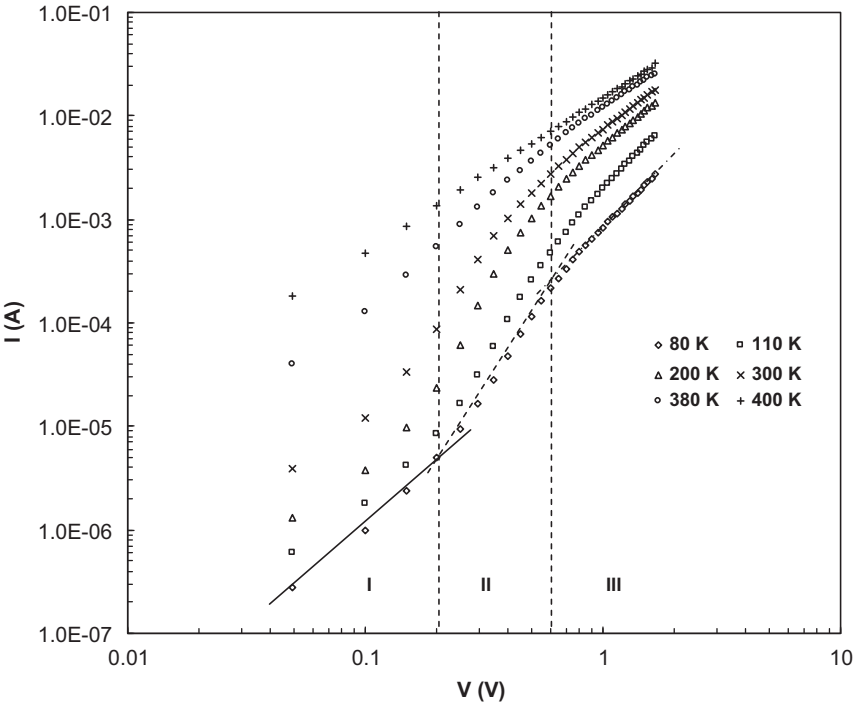

Fig. 7. A double logarithmic forward bias *I–V* plot of the Au/TiO_2/n-Si SBD at six different temperatures.

interface, which often immobilizes the injected charge carriers, are important factors that govern the SCLC mechanism. The strong temperature dependence of ideality factor in the Au/TiO_2/n-Si SBD shows that the current process occurring in the structure would be a possible alternative candidate in determining the forward current at the intermediate and high bias voltages. As a result, we can say that the region-I shows an ohmic behavior at low bias voltages, the region-II the TCLC behavior, and the region-III SCLC behavior in Au/TiO_2/n-Si SBD. Also, as can be seen from Fig. 7, at high temperatures ($T \geq 380$ K) the TE theory may dominate rather than the other current transport mechanisms.

4. Conclusion

In this study, forward and reverse-bias *I–V* characteristics of Au/TiO_2/n-Si (SBD) were measured in the temperature range of 80–400 K. While the zero-bias barrier height ϕ_{B0} increased and ideality factor n decreased with increasing temperature. ϕ_{B0} versus $q/2kT$ is an evidence of a Gaussian distribution of the BHs in two temperature ranges. So that, this temperature behavior of the Au/TiO_2/n-Si (SBD) has been attributed to the barrier inhomogeneities at the M/S interface. Also, the experimental results of ϕ_{B0} and n_{ap} fit very well with the theoretical equations related to the double Gaussian distribution. This result suggests that experimental data of Au/TiO_2/n-Si (SBD) can be satisfactorily explained by assuming the two Gaussian distributions of the Schottky barrier heights in the temperature range of 80–400 K, suggesting that the contacts are not spatially uniform. The Richardson constant values of 121.01 A/cm^2 K^2 (200–400 K) and 324.06 A/cm^2 K^2 (80–170K) were obtained by means of the modified Richardson plot considering.

Acknowledgments

This study was supported by the Turkish Prime Ministry state Planning Agency under project no: 2001K120590 and G.U BAP project no: 05/2008-11.

References

[1] Karunagara B, Kim Kyunghae, Mangalaraj D, Yi Junsin, Velumani S. Sol. Energy Mater. Sol. Cells 2005;88:199.
[2] Jeong BS, Norton DP, Budai JD. Solid-State Electron. 1991;34:531.
[3] Zeman P, Takabayashi S. Surf. Coat. Technol. 2002;153:93.
[4] Okimura K. Surf. Coat. Technol. 2001;135:286.
[5] Mardare D, Rusu GI. Mater. Sci. Eng. B 2000;75:68.
[6] Ishikawa Y, Matsumoto Y. Electrochim. Acta 2001;46:2819.
[7] Mornis Henry B, US patent no.: 4200474, 1978.
[8] Kozlowski MR, Tyler PS, H: Smyrl W, Atanasoki RT. J. Electrochem. Soc. 1989;136:4949.
[9] Lottiaux M, Boulesteix C, Nihoul G, et al. Thin Solid Films 1989;170:107.
[10] Yeung KS, Lam YW. Thin Solid Films 1983;109:405.
[11] Williams LM, Hess DW. J. Vac. Sci. Technol. A 1983;1:1810.
[12] Vorotilov KA, Orlova EV, Petrovsky VI. Thin Solid Films 1992;207:180.
[13] Gartner M, Parlog C, Osiceanu P. Thin Solid Films 1993;234:561.
[14] Suhail MH, Mohan Rao G, Mohan S. J. Appl. Phys. 1993;71(3) 1421.
[15] Meng LJ, Andritschky M, dos Santos MP. Thin Solid Films 1993;223:242.
[16] Meng LJ, dos Santos MP. Thin Solid Films 1993;226:22.
[17] Tang H, Prasad K, Sanjines R, Schmid PE, Levy F. J. Appl. Phys. 1994;75(4):2042.
[18] Biber M. Physica B 2003;325:138.

[19] Akkal B, Benamara Z, Bideux L, Gruzza B. Microelectron. J. 1999;30:673.
[20] Cova P, Singh A. Solid-State Electron. 1990;33:11.
[21] Mönch W. J. Vac. Sci. Technol. B 1999;17:1867.
[22] Chand S, Kumar J. Semicond. Sci. Technol. 1996;11:1203.
[23] Chand S, Kumar J. Appl. Phys. A 1997;65:497.
[24] Karataş Ş, Altındal Ş, Türüt A, Özmen A. Appl. Surf. Sci. 2003;217:250.
[25] Gümüş A, Türüt A, Yalçın N. J. Appl. Phys. 2002;91:245.
[26] Karataş Ş, Altındal Ş, Çakar M. Physica B 2005;357:386.
[27] Tung RT. Phys. Rev. B 1992;45:13509.
[28] Song YP, Van Meirhaeghe RL, Laflere RL, Cordon F. Solid-State Electron. 1986;29:633.
[29] Werner JH, Guttler HH. J. Appl. Phys. 1991;69:1522.
[30] Chand S, Kumar J. Semicond. Sci. Technol. 1996;11:1203.
[31] Osvald J, Horvarth ZJ. Appl. Surf. Sci. 2004;234:349.
[32] Çetin H, Ayyildiz E. Semicond. Sci. Technol. 2005;20:625.
[33] Karataş Ş, Altındal Ş. Mater. Sci. Eng. B 2005;122:133.
[34] Horvarth ZJ. Solid-State Electron. 1996;39:176.
[35] Rossi RC, Tan MX, Lewis NS. Appl. Phys. Lett. 2000;77(17):2698.
[36] Sze SM. Physics of Semiconductor Devices, second ed. New York: Wiley; 1981.
[37] Card HC, Rhoderick EH. J. Phys. D: Appl. Phys. 1971;4:1589.
[38] Rhoderick EH, Williams RH. Metal-Semiconductor Contacts. Oxford: Clarendon; 1988.
[39] kampen TU, Park S, Zahn DRT. Appl. Surf. Sci. 2002;190:461.
[40] Bolognesi A, Di. Carlo A, Lugli P, Kampen T, Zahn DRT. J. Phys.: Condens. Matter 2003;15:2719.
[41] Singh A, Reinhhardt KC, Anderson WA. J. Appl. Phys. 1990;68(7): 3475.
[42] Card HC, Rhoderick EH. J. Phys. D: Appl. Phys. 1971;4:1589.
[43] Tung RT. Phys. Rev. B 1992;45:13509.
[44] Schmitsdorf RF, Kampen TU, Mönch W. Surf. Sci. 1995;324:249.
[45] Chand S, Bala S. Appl. Surf. Sci. 2005;252:358.
[46] Özdemir AF, Turut A, Kökçe A. Semicond. Sci. Technol. 2006;22:298.
[47] Pakma O, Serin N, Serin T, Altındal Ş. J. Appl. Phys. 2008;104: 014501.
[48] Ahmad Z, Sayyad MH. Physica E 2009;41:631.
[49] Shafai TS, Anthopoulos TD. Thin Solid Films 2001;398–399:361.
[50] Jafar MMA. Semicond. Sci. Technol. 2003;18:7.
[51] Aydogan S, Güllü Ö, Türüt A. Phys. Scr. 2009;79:035802.
[52] Chowdhury P, Barshilia HC, Selvakumar N, Deepthi B, Rajam KS, Chaudhuri AR, et al. Physica B 2008;403:3718.
[53] Gupta RK, Ghosh K, Kahol PK. Curr. Appl. Phys. 2009;9:933.